South African Journal of Botany 120 (2019) 219–229

Contents lists available at ScienceDirect

South African Journal of Botany

journal homepage: www.elsevier.com/locate/sajb

Effects of hydroxycinnamic acids on the glycolysis pathway

J. Serina, M.X. Fernandes, P.C. Castilho *

Centro de Química da Madeira, University of Madeira, Campus da Penteada 9020-105, Madeira Island, Portugal

ARTICLE INFO

Article history:
Received 30 March 2018
Received in revised form 1 June 2018
Accepted 18 June 2018
Available online 7 July 2018

Edited by A Mocan

Keywords:
Hydroxycinnamic acids
Molecular docking
Enzyme inhibition
In vitro kinetic assays
Glycolysis

ABSTRACT

Glycolysis is a metabolic pathway vital to the production of energy and some organisms rely on it solely to meet their energy requirements. It is also a central pathway in the metabolism of carbohydrates and a source of therapeutic targets against diabetes and cancer. Caffeoylquinic acids (CQAs) have been extensively studied for their role in the treatment and prevention of diabetes (and cancer) but their mechanisms of action remain mostly unknown. As such, molecular docking was used to find possible targets of CQAs in the glycolysis pathway. The molecular docking assays showed that CQAs were docked preferably to the Rossman fold (nicotinamide adenine dinucleotide — NAD(H) binding site) of oxidoreductases, that use NAD(H) as a cofactor, than to any other site. *In-vitro* assays were then performed using two NAD(H) dependent oxidoreductases from glycolysis (alcohol dehydrogenase and L-lactate dehydrogenase) in order confirm if CQAs would compete with the cofactor to inhibit the reaction. The results from these assays indicate that CQAs can act as both inhibitors and activators of NAD(H) dependent oxidoreductases of the glycolysis pathway.

1. Introduction

Glycolysis was the first major metabolic pathway to be fully understood (Lenzen, 2014). This pathway has many steps that ultimately lead to the catabolism of glucose and other hexoses into pyruvate (Pelicano et al., 2006; Bar-Even et al., 2012). Once pyruvate is produced, the pathway diverges depending on the availability of oxygen. If it is available, pyruvate molecules are oxidized to carbon dioxide and water. If oxygen is not available, pyruvate is reduced to lactic acid. By reducing pyruvate, NADH (nicotinamide adenine dinucleotide) is converted to NAD^+ (Pelicano et al., 2006; Bolaños et al., 2010; Bar-Even et al., 2012). NAD^+ is a cofactor for many of the enzymes in glycolysis such as alcohol dehydrogenase (EC 1.1.1.1), aldehyde dehydrogenase (EC 1.2.1.5) and glyceraldehyde 3-phosphate dehydrogenase (EC 1.2.1.12). Some enzymes use nicotinamide adenine dinucleotide phosphate (NADP(H)) instead of NAD^+ but both have the same function (Bolaños et al., 2010). The complete glycolysis pathway, as well as its connections to other metabolic pathways, can be seen in Fig. 1.

Not all enzymes present in Fig. 1 are expressed in humans and in some cases where there are several enzymes for a single reaction, the enzymes belong to different cell types. As an example, the reaction that converts α-D-glucose to α-D-glucose-6-phosphate is catalyzed by two enzymes for eukaryotes (2.7.1.1 and 2.7.1.2) and two enzymes for Archaea bacteria (2.7.1.63 and 2.7.1.147).

As this work belongs to a larger project, in which one of the goals is to find new treatments and molecular targets for Diabetes mellitus, only enzymes expressed in humans were considered for evaluation through the methods described on this manuscript.

1.1. Enzymes

1.1.1. EC 1.1.1.1 – Alcohol dehydrogenase

Alcohol dehydrogenase (ADH) is an enzyme that belongs to the medium-chain dehydrogenase/reductases (MDR) super family. It is a zinc containing MDR expressed by nine different genes in the human genome to form five classes of ADHs (I to V). Classes I and II are found mainly in the liver (Niederhut et al., 2001; Venkataramaiah and Plapp, 2003). Class I ADHs account for three of these genes due to the encoding of three different subunits: α or A which is the only one expressed during the fetal phase, β or B whose expression begins before birth and γ or C which is expressed after birth (Niederhut et al., 2001). The subunits encoded by these genes can form homo or heterodimers while classes II through V only form homodimers (Niederhut et al., 2001). This makes ADH the most common MDR in humans (Nordling et al., 2002a, 2002b). In ADHs a distinction is also made between Class III and non-Class III enzymes as the former are formaldehyde-active while the latter are ethanol-active (Niederhut et al., 2001; Nordling et al., 2002a, 2002b). An increased activity of Class III isoenzymes is found in patients with pancreatic cancer (Jelski et al., 2014) and pancreatitis (Jelski et al., 2011). Heavy drinkers with either of these conditions will also exhibit a higher activity of Class I ADH.

The activity of ADH can be reduced through several common medications such as aspirin (acetylsalicylic acid) and salicylic acid

* Corresponding author.
E-mail address: castilho@uma.pt (P.C. Castilho).

https://doi.org/10.1016/j.sajb.2018.06.016
0254-6299/

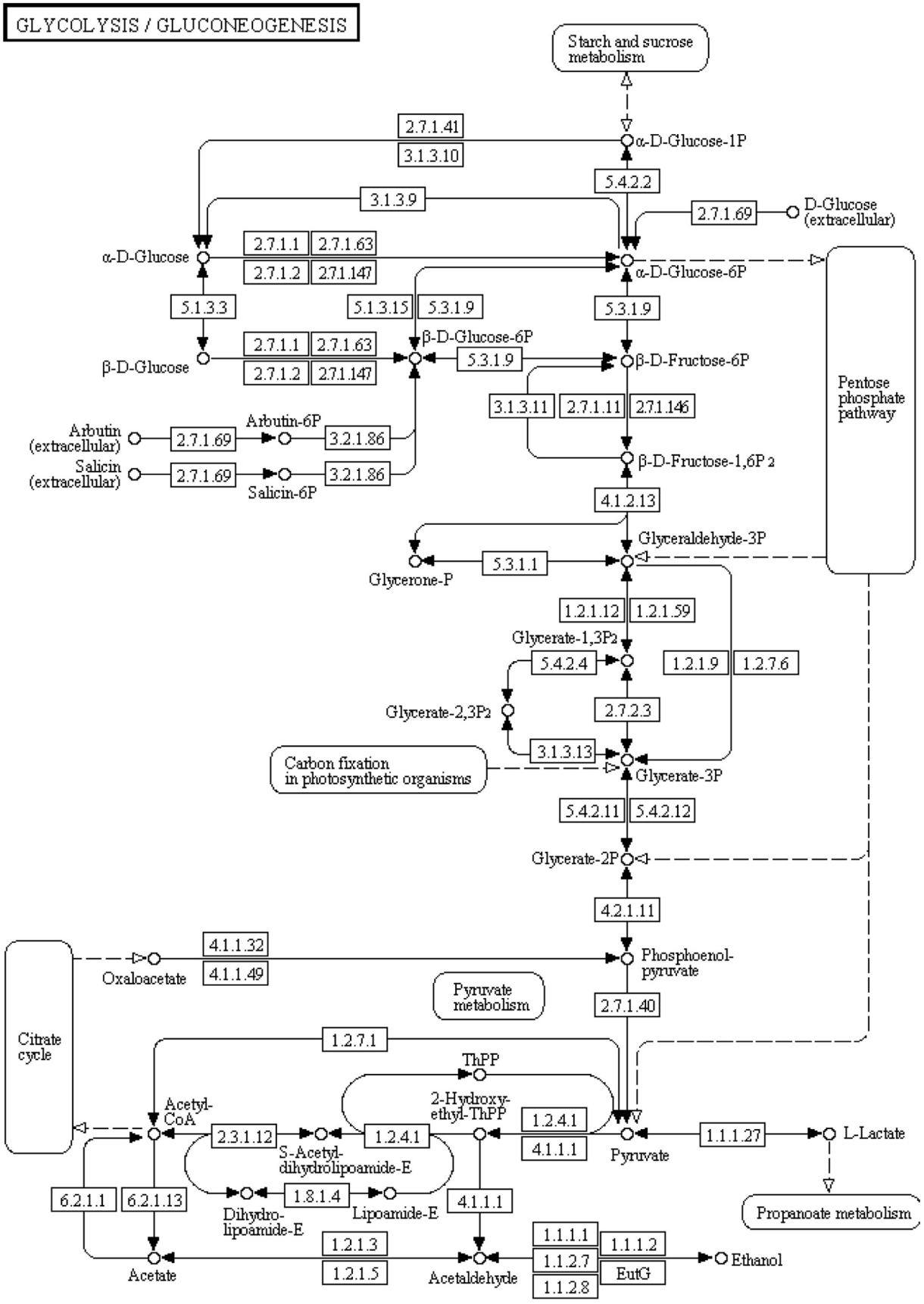

Fig. 1. The glycolysis metabolic pathway from KEGG (Ogata et al., 1999; Kanehisa et al., 2016, 2017).

(Lee et al., 2015), acetaminophen (paracetamol) (Lee et al., 2013) and cimetidine (Lai et al., 2013). Of the four compounds, the one that affects the catalytic activity of Class II ADH the most is cimetidine. With a concentration of 1 mM, cimetidine inhibited the activity by approximately 75% at 50 mM of ethanol.

Formamides are also effective inhibitors of ADH enzymes as they mimic their aldehyde products. However, formamides act through non-competitive inhibition against alcohols, allowing them to inhibit ADHs even in high concentrations of alcohols (Venkataramaiah and Plapp, 2003; Gibbons and Hurley, 2004). Haseba and colleagues (Haseba et al., 2008), also studied the inhibition of ADHs (in mice) using polyphenols present in whisky and found that vanillin, syringaldehyde and ellagic acid inhibit ADH class I through mixed inhibition while caffeic acid inhibited it through competitive inhibition. Caffeic acid, performed the best out of these four compounds with an inhibition constant of 0.08 μmol/L while pyrazone, a well-documented inhibitor of ADH had an inhibition constant of 5.1 μmol/L. Additionally, Cao and colleagues (Cao et al., 2010) report that ADH from *Lactococcus lactis* is competitively inhibited by both ATP and ADP with a synergetic effect between the two molecules and hypothesize that this inhibition serves as a regulatory mechanism in the production of ATP.

1.1.2. EC 1.1.1.27 — L-lactate dehydrogenase

L-lactate dehydrogenase (LDH — EC 1.1.1.27) is responsible for converting lactic acid to pyruvate and *vice-versa* using NAD^+ or NADH as a cofactor. Its catalytic mechanism has been studied in depth and occurs in three stages, the first stage involves the binding of the cofactor, followed by the binding of the substrate and the mechanism is concluded by the closure of the active site (Quaytman and Schwartz, 2009). Despite having a well-defined mechanism, the order of the several transition states and chemical steps varies depending on the organism (Quaytman and Schwartz, 2009). Like ADH, LDH is inhibited by ADP and ATP in *L. lactis* (Cao et al., 2010).

There are two genes that encode LDH, *LDHA* and *LDHB*. The proteins expressed by these two genes form tetramers that vary from only LDHA (isoenzyme LDH5) to only LDHB (isoenzyme LDH1). LDHA has a higher affinity for pyruvate than LDHB and is expressed mainly in tissues that perform glycolysis heavily such as skeletal muscles. LDH has become a target in oncology treatment due to its over expression and increased activity in cancer cells (Feron, 2009; Doherty and Cleveland, 2013).

The over stimulation of anaerobic glycolysis in cancer cells is known as the Warburg effect (Feron, 2009; Doherty and Cleveland, 2013) described by the first time in 1956 by Otto Warburg (Warburg, 1956). This effect is driven by hypoxia that, can be induced by cancer cells in healthy cells through the endocytosis of hydrogen peroxide (Doherty and Cleveland, 2013). Lactate from hypoxic cancer cells is exported to non-hypoxic cancer cells that oxidize it and complete aerobic respiration. This symbiotic effect allows hypoxic cells to survive otherwise apoptotic conditions (very low pH) and provides energy to all cancer cells (Doherty and Cleveland, 2013). This increased rate of glycolysis is favored instead of aerobic respiration despite the lower energy yield since the conversion of lactate to pyruvate produces sufficient NAD^+ to fuel glycolysis if glucose is available. This also allows cancer cells to fuel the pentose phosphate and fatty acid synthesis pathways that are pivotal for fast cellular replication (Feron, 2009; Doherty and Cleveland, 2013). Lactic acid is also considered a bio-marker for metastasis (Walenta and Mueller-Klieser, 2004).

Gossypol is a polyphenol extracted from cotton seed which has been extensively studied for its male contraceptive properties. It is also known that gossypol is a non-selective inhibitor of NAD(H) binding to oxidoreductases and the inhibition of LDH-C which is expressed only in the testes and sperm (Yu et al., 2001). Additionally, it has also been studied as the starting point for several anti-malaria drugs since *Plasmodium falciparum* relies heavily on LDH for energy production (Conners et al., 2005; Wiwanitkit, 2007).

2. Material and methods

In this work, molecular docking was used as a screening technique to narrow down the number of potential molecular targets and to predict the mechanism of inhibition to be tested later through *in-vitro* tests. This is similar to the approach of Zengin et al. (2017) although the authors used molecular docking after establishing inhibitory potency *in-vitro*.

2.1. Molecular docking

The first step of this work was to determine which glycolysis enzymes (Fig. 1) are expressed in humans so that their crystal structure files could be downloaded from the PDB database and prepared for the docking assays. Of the 31 enzymes expressed in humans, 9 did not have a structure file on the PDB data base when the molecular docking assays were performed. Of the remaining 21, one of the enzymes (EC 2.7.1.11) had a very poor resolution (6.0 Å) and as such was not used.

The same method was applied to all enzymes. Briefly, a holoenzyme structure file was downloaded from the PDB database for each of the 20 enzymes studied. Each structure file was then prepared for docking using AutoDock Tools (Morris et al., 2009). First, water molecules and any other molecules/ligands were removed until only the enzyme remained, hydrogen atoms were added and finally, charges were assigned to each atom. The new structure was then saved so it that could be used later for docking with AutoDock Vina (Trott and Olson, 2010). Then, the structure of any other ligands (cofactors, substrates, products or inhibitors) from the crystal structure was isolated and prepared for docking through the same method as the enzymes and then saved individually.

Six caffeoylquinic acids (1,3-diCQA; 1,5-diCQA; 3,4-diCQA; 3,4-diCQA; 4,5-diCQA and 5-CQA, Fig. 2) were also prepared for docking using the same method described in a previous work of the group (Serina et al., 2016). Briefly, the molecules were created and optimized using the MM + forcefield to an RMS below 0.01 kcal/mol. After the optimization, each CQA molecule was prepared for docking through the same procedure as the enzymes in AutoDock Tools.

Once all ligands (CQAs and ligands present in the enzyme crystal structure) were prepared for docking, the first set of the molecular docking experiments were performed (rigid targeted/localized molecular docking) using AutoDock Vina (Trott and Olson, 2010). On this set, the docking search area was defined as a cube with 26 Å sides centered at the center of mass for each non-enzyme ligand from the crystal structure. The ligands from each enzyme's structure were redocked to their site on the enzyme to evaluate their binding affinity. The affinity of these ligands was only considered when their docked conformation matched the conformation of the crystal structure. This affinity was then used as a benchmark to evaluate the CQA's potential effect. This was done for each chain of the enzyme in the file even if several chains contained the same ligands. Then, each CQA was docked at all the relevant sites for each enzyme (co-factor site, substrate/product site and allosteric inhibitor/regulatory sites if present).

The second stage of the molecular docking studies was a series of blind docks. In these experiments, each CQA was docked to the enzyme but instead of limiting the docking search area to the area around the target site, the docking area was expanded to encompass the entire enzyme to verify if the CQAs would indeed bind to the target sites of the enzyme. This step of the molecular docking assays removed any bias from the results that might have arisen from docking the CQAs directly to the target sites.

Finally, the CQAs that were docked to the same site on the first two stages of the docking experiments were used in a third docking stage, flexible docking. To establish the docking search area for these calculations, the ligand from that site was selected in the original crystal structure. Then, all enzyme atoms around 8 Å of the

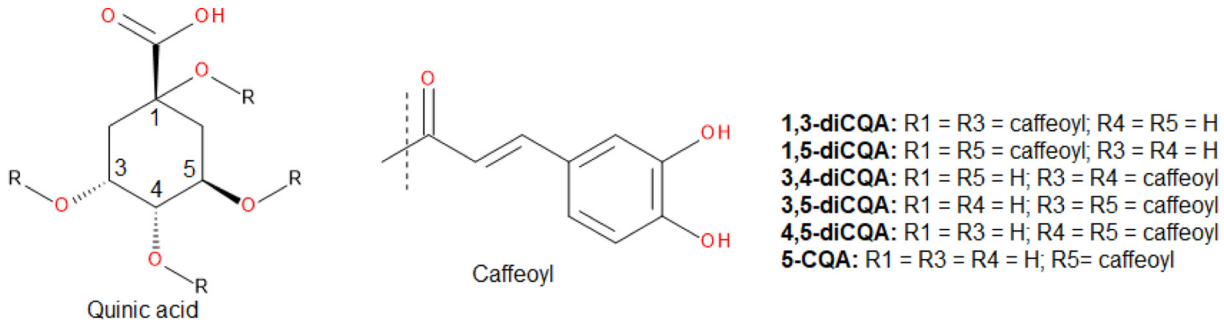

Fig. 2. Caffeoylquinic acids studied in this paper.

ligand were selected to find any atoms that could establish any intermolecular interactions. At this point, the selection of enzyme atoms was expanded to include the residue they belonged to. Finally, the docking area was established as the volume capable of accommodating all the selected residues and allows their bonds to rotate while remaining inside the search area.

During this third and final docking stage, the CQAs with the best (most negative) affinity were docked at their best scoring site but with flexible enzyme residues. This type of docking allows both the ligand and the enzyme's bonds to rotate to achieve the best possible conformation for both the enzyme (receptor) and the CQA (ligand). Although extremely lengthy and resource intensive (over one week for each CQA / site combination), this type of docking also provides the most accurate results (closest to *in-vivo*/*in-vitro* conditions) as it can rearrange the conformation of the receptor to better accommodate to the presence of the ligand.

Due to the limited amount of diCQAs available, it would only be possible to use each diCQA for the kinetic assays of one enzyme. A third CQA, 5-CQA was used on both assays as its availability was not as limited as the diCQAs and it would serve as a relative benchmark since it always scored the poorest of all CQAs in the molecular docking studies. As such, two enzymes that were predicted to be inhibited by different diCQAs were chosen for the *in-vitro* assays (alcohol dehydrogenase and lactate dehydrogenase).

2.2. In-vitro assays

The *in-vitro* assays had two goals, the first was to validate the results from molecular docking through enzyme kinetic assays and the second was to establish the IC50 of each CQA towards each enzyme. In the enzyme kinetic assays, the concentration of the cofactor or the substrate was varied and the concentration of the CQA was maintained while in the IC50 assays, the concentration of the cofactor and the substrate were fixed and the concentration of CQA was varied.

While in the molecular docking, the enzymes studied were all from humans, for the *in-vitro* assays the enzymes used were not from humans. Although there are some small differences in the sequence and structure between the human and non-human enzymes, considering that this is mainly an exploratory study and that the predicted/target site of the compounds is the highly conserved Rossman Fold (NAD(H) binding site), these differences were considered minor and, non-human enzymes were used in the *in-vitro* assays.

2.2.1. Alcohol dehydrogenase (EC 1.1.1.1)

2.2.1.1. Materials. Ethanol active alcohol dehydrogenase from *Saccharomyces cerevisiae*, NAD^+, 5-caffeoyquinic acid and bovine serum albumin (BSA) was acquired from Sigma-Aldrich. Ethanol was acquired from Fisher, disodium phosphate from Merck and phosphoric acid from DBH. Both 1,3 and 1,5-dicaffeoylquinic acids were acquired from Chengdu Biopurity Phytochemicals.

2.2.1.2. Method. The measurements of enzyme activity were performed in a Perkin Elmer multilabel plate reader Victor 3 on 96 well cyclic olefin copolymer plates at 340 nm. Buffer solutions of 10 and 60 mM of disodium phosphate were prepared, and their pH was reduced to 7.5 and 8.5 respectively with a solution of 8% phosphoric acid. The 10 mM buffer was used to prepare the initial concentrated enzyme solution (≈1 mg/mL) and the enzyme diluent solution (0.1% BSA w/v) in 10 mM Na_2HPO_4 at pH 7.5. The concentrated enzyme solution was diluted (1:125) using the diluent solution and was kept between 2 and 8 °C. The NAD^+ and caffeoylquinic acid solutions were also kept at this temperature and were stable for long periods of time (over three weeks). The method used is a slightly modified version of the protocol proposed by Taber (Taber, 1998). Briefly, 100 μL of disodium phosphate buffer at pH 8.5 (60 mM) was mixed with 0–8 μL of ethanol solution (3 M), 0–10 μL of NAD^+ (15 mM), 0–40 μL of 1,3 or 1,5-di-caffeoylquinic acid (0.25 mg/mL ≈ 0.48 mM) or 0–50 μL of 5-caffeoylquinic acid (1 mM), 20 μL of diluted enzyme solution (approximately 5 U/mL) and water to complete a volume of 300 μL. In all assays, the reaction was started by adding the enzyme to each well and absorbance was measured at 340 nm every minute for 10 min. For each variable concentration (cofactor, substrate or CQA) there were seven repetition wells. Once the data was collected, the highest and the lowest (absorbance) values of each concentration (set of seven wells) were discarded. The average of the remaining five wells was calculated and used as the absorbance for that concentration. The velocity of the reaction was then calculated using the following formula: $\frac{A_{340\ nm}t2 - A_{340\ nm}t1}{t_2 - t_1}$ where t_2 and t_1 represent the time (in this case 5 and 0 min) and where $A_{340\ nm}t2$ and $A_{340\ nm}t1$ represent the average (n = 5) absorbance at time t2 and t1.

2.2.2. Lactate dehydrogenase (EC 1.1.1.27)

2.2.2.1. Materials. NAD^+, 5-caffeoyquinic acid and bovine serum albumin (BSA) were acquired from Sigma-Aldrich. Lactate dehydrogenase from rabbit muscle was acquired from Roche. Calcium lactate pentahydrate, ethylenediaminetetraacetic acid dihydrate (EDTA) and disodium phosphate were acquired from Merck. Phosphoric acid was acquired from DBH and both 3,4 and 3,5-dicaffeoylquinic acids were acquired from Chengdu Biopurity Phytochemicals.

2.2.2.2. Method. The measurements of enzyme activity were performed in a Perkin Elmer multilabel plate reader Victor 3 on 96 well cyclic olefin copolymer plates at 340 nm. Buffer solutions of 200 and 100 mM of disodium phosphate were prepared, and their pH was reduced to 8.5 and 7.5 respectively with a solution of 8% phosphoric acid. The 100 mM buffer was used to prepare the enzyme solution (≈11 U/mL) with 0.1% BSA (w/v). The solution was kept between 2 and 8 °C. The NAD^+ and CQA solutions were also kept at

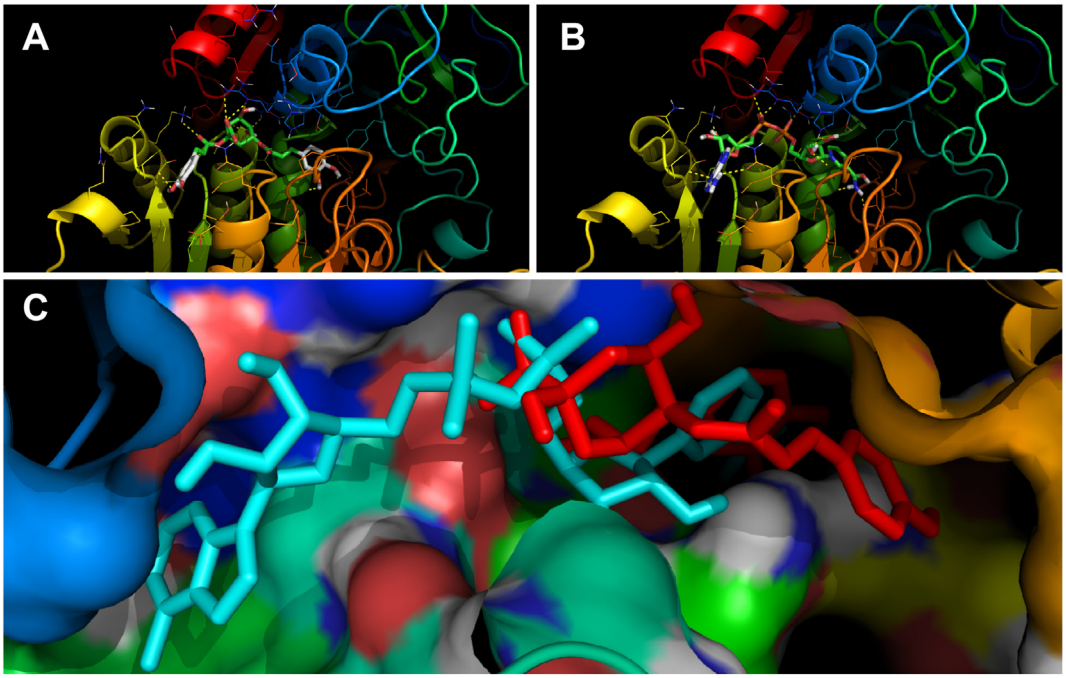

Fig. 3. A) 1,3-diCQA docked at NAD site of ADH; B) NAD binding from the crystal structure of ADH (PDB id: 1U3W); C) NAD (cyan) from the crystal structure of LDH (PDB id: 4M49) and 3,4-diCQA (red) docked at the NAD binding site of LDH. (For interpretation of the references to color in this figure legend, the reader is referred to the web version of this article.)

this temperature and were stable for long periods of time (over three weeks). The method used is a slightly modified version of the protocol proposed by Powers et al. (2007). Briefly, 100 μL of disodium phosphate buffer at pH 8.5 (200 mM) was mixed with 0–20 μL of calcium lactate (50 mM) + EDTA (75 mM) solution, 0–10 μL of NAD+ (15 mM), 0–40 μL of 1,3 or 1,5-di-caffeoylquinic acid (0.25 mg/mL) or 0–50 μL of 5-caffeoylquinic acid (1 mM), 20 μL of enzyme solution and water to complete a volume of 200 μL. In all assays, the reaction was started by adding the enzyme to each well and absorbance was measured at 340 nm every minute for 10 min. For each variable concentration (co-factor, substrate or CQA) there were seven repetition wells. Once the data was collected, the highest and the lowest (absorbance) values of each concentration (set of seven wells) were discarded. The average of the remaining five wells was calculated and used as the absorbance for that concentration. The velocity of the reaction was then calculated using the following formula: $\frac{A_{340\ nm}t2-A_{340\ nm}t1}{t_2-t_1}$ where t_2 and t_1 represent the time (in this case 5 and 0 min) and where $A_{340\ nm}t2$ and $A_{340\ nm}t1$ represent the average (n = 5) absorbance at time $t2$ and $t1$.

EDTA was added to the calcium lactate solution to prevent the formation of calcium pyrophosphates that precipitated when the calcium lactate was mixed with the disodium phosphate buffer.

3. Results

3.1. Molecular docking

The docking results (full data not shown) revealed that in oxidoreductases (enzymes classified as EC 1) that use NAD(H) as a

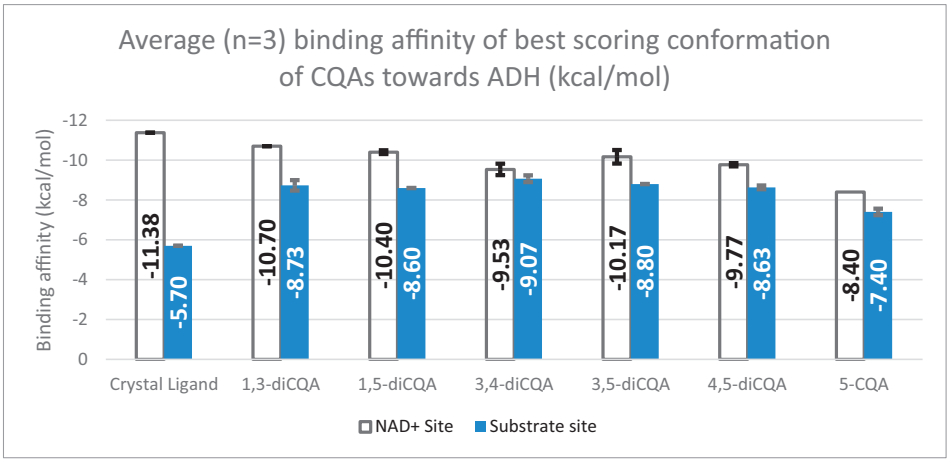

Fig. 4. Average (n = 3) binding affinity of best scoring conformation of CQAs towards ADH (kcal/mol).

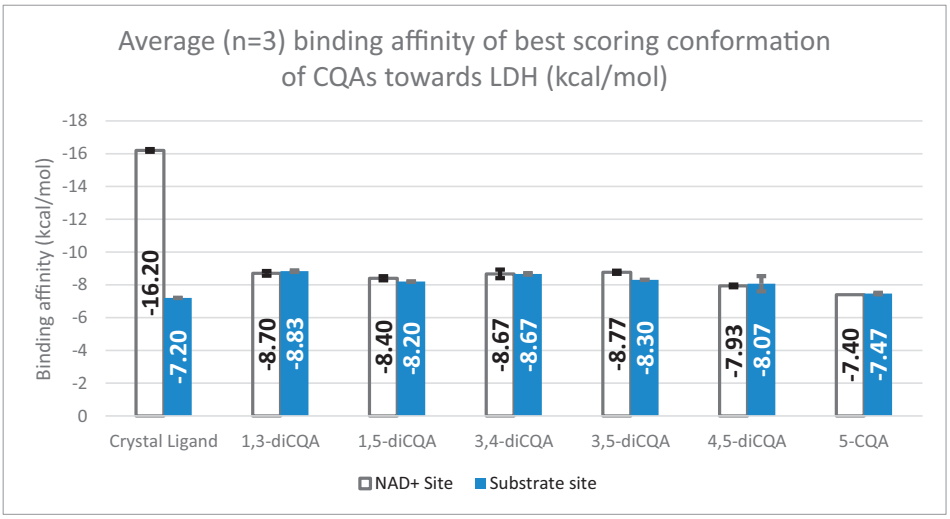

Fig. 5. Average (n = 3) binding affinity of best scoring conformation of CQAs towards LDH (kcal/mol).

cofactor, diCQAs were biding preferably to the NAD(H) site over any other site on the enzyme. Considering the docking results and the limited availability of diCQAs two enzymes of this type that were potentially inhibited by different CQAs were chosen for the *in-vitro* assays. The enzymes selected for *in-vitro* assays were alcohol dehydrogenase and lactate dehydrogenase. In Fig. 3, the binding of CQAs to NAD^+'s binding site is observable both for both enzymes studied in this paper.

As shown in Fig. 3(A and B), the carboxylic acid group from CQAs interacts with the same positively charged residues as the phosphate groups from NAD(H) while the diphenol rings from the caffeic acid moieties mimic the nicotinamide and adenine aromatic rings and establish hydrogen bonds with some of the same residues as the amides from NAD(H).

The average (n = 3) binding affinity for the best scoring conformation of each CQA regarding ADH and LDH as well as their respective crystal structure ligands can be found in Figs. 4 and 5.

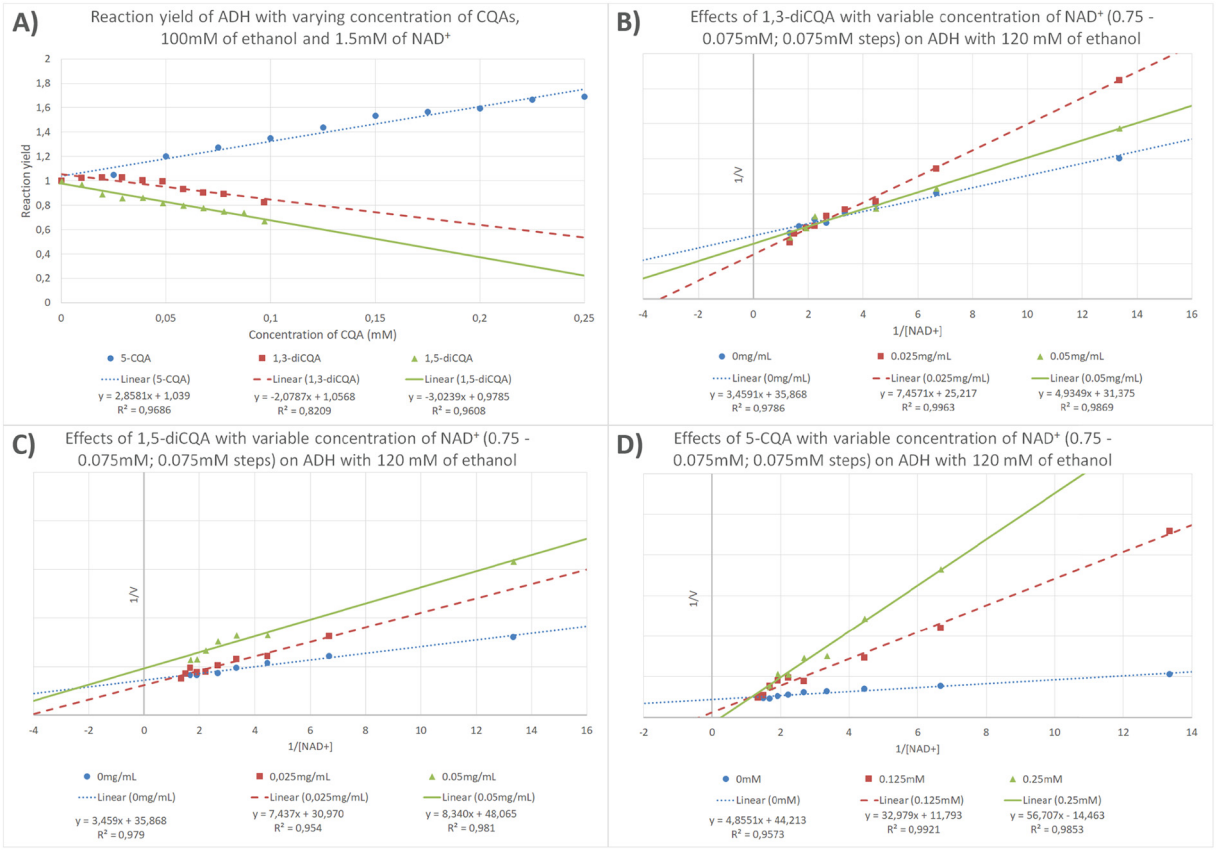

Fig. 6. Effects of CQAs on ADH and NAD^+ Kinetics: A) Reaction yield with varying concentration of CQAs with 100 mM of Ethanol and 1.5 mM of NAD^+; B) Effects of 1,3-diCQA with variable concentration of NAD+ (0.75–0.075 mM; 0.075 mM steps) on ADH with 120 mM of ethanol; C) Effects of 1,5-diCQA with variable concentration of NAD+ (0.75–0.075 mM; 0.075 mM steps) on ADH with 120 mM of ethanol; D) Effects of 5-CQA with variable concentration of NAD+ (0.75–0.075 mM; 0.075 mM steps) on ADH with 120 mM of ethanol.

3.2. In-vitro assays

The kinetic data of each enzyme were recorded and represented using Lineweaver-Burk plots (Lineweaver and Burk, 1934). This type of plot represents the inverse of the reaction velocity over the inverse of the concentration of studied substrate. This type of plot makes it possible to identify the mechanism of inhibition towards each substrate. When the regressions of the data points intercept on the abscissa (xx or horizontal axis) this means that inhibitor is non-competitive while, if the interception is on the ordinate (yy or vertical axis) the inhibitor is competitive regarding the substrate. If the interception is between the ordinate and the abscissa, the inhibition is considered as mixed (partially competitive and partially non-competitive) and if the regressions of the data points are parallel there is no inhibition. Due to experimental errors, the interception of the regressions for competitive and non-competitive inhibitors does not always perfectly overlap with the corresponding axis. Experimental errors can also lead to several interception points instead of one.

3.2.1. Alcohol dehydrogenase

One of the goals of the *in-vitro* assays was to measure the IC50 of each CQA towards ADH (Fig. 6 - A) and to investigate their inhibition mechanism. Due to the reduced amount of diCQAs, it was not possible to establish their IC50. While 1,3-diCQA achieved an inhibition of approximately 17.7% with 0.05 mg/mL, 1,5-diCQA achieved an inhibition of approximately 32.9% at the same concentration. On the other hand, 5-CQA acted as an activator. While the effects of 1,5-diCQA and 5-CQA had a good regression coefficient ($R^2 > 0.96$), 1,3-diCQA had an acceptable regression coefficient ($R^2 > 0.82$). Due to linearity between the concentration of the compounds and their effect on the yield of the reaction, it is possible to easily estimate the IC50 for the diCQA and the concentration of 5-CQA that increased the reaction yield by 50%.

Considering the data from Fig. 6 – A) and the equation for the effect of 5-CQA on the reaction yield ($y = 2.8581x + 1.039$), it is possible to calculate that concentrations of approximately 0.16 and 0.336 mM can increase the reaction's yield by 50 and 100% respectively.

Considering the equations for 1,3-diCQA and 1,5-diCQA ($y = -2,0787x + 1,0568$ and $y = -3,0239x + 0,9785$ respectively) it is possible to estimate that the IC50 for these compounds is approximately 0.268 mM for 1,3-diCQA and 0.158 mM for 1,5-diCQA.

When analyzing the initial assay of the effect of 1,3-diCQA on NAD^+ kinetics (data not shown), there was good linearity at the tested concentrations (0, 0.025 and 0.05 mg/mL). However, the linear regressions of each concentration intercepted each other in the first quadrant of the Lineweaver–Burk plot. Furthermore, the linear regression for the lower concentration of 1,3-diCQA had a higher slope than the higher concentration of 1,3-diCQA which would indicate that the lower concentration had a stronger inhibitory effect on the reaction. These unexpected results were initially attributed to some form of experimental error and the assay was repeated. The data from the repetition can be seen on (Fig. 6 – B). Once again, all linear regressions had a very good regression coefficient ($R^2 > 0.95$), intercepted in the first quadrant of the plot and the regression for the lower concentration of 1,3-diCQA had a higher slope that the higher concentration.

Unlike 1,3-diCQA, 0.05 mg/mL of 1,5-diCQA had a stronger inhibitory effect (higher slope) than 0.025 mg/mL (Fig. 6 – C). Additionally, the interception of the linear regressions is not a single point. While the regressions for 0 and 0.025 mg/mL of 1,5-diCQA intercept in the first quadrant the regressions for 0 and 0.05 mg/mL intercept in the second quadrant (characteristic of mixed inhibition).

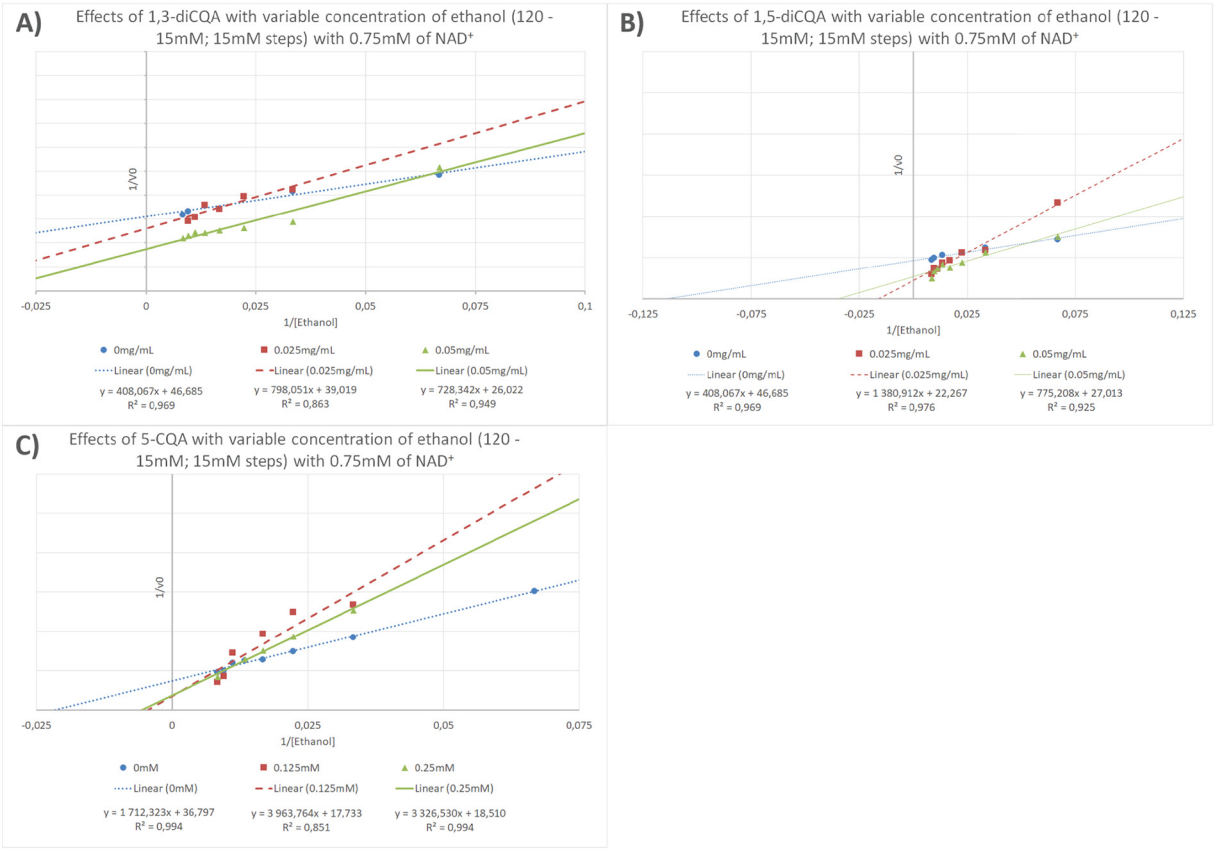

Fig. 7. Effects of CQAs on ADH and ethanol Kinetics: A) Effects of 1,3-diCQA with variable concentration of ethanol (120–15 mM; 15 mM steps) with 0.75 mM of NAD^+; B) Effects of 1,5-diCQA with variable concentration of ethanol (120–15 mM; 15 mM steps) with 0.75 mM of NAD^+; C) Effects of 5-CQA with variable concentration of ethanol (120–15 mM; 15 mM steps) with 0.75 mM of NAD^+.

When evaluating the effects of 5-CQA towards the binding of NAD^+ (Fig. 6 — D), the expected behavior is observed for increasing concentrations of inhibitor.

Higher concentrations of 5-CQA led to a higher slope on the regression. However, the interception of the regressions is once again in the first quadrant.

When evaluating the effects of these ligands with varying concentrations of ethanol, both 1,3 and 1,5-diCQA had a higher inhibitory activity at 0.025 mg/mL than at 0.05 mg/mL (Fig. 7 — A and B respectively).

In Fig. 7 — A it is possible to observe that 0.025 mg/mL has a stronger inhibitory power (higher slope) than 0.05 mg/mL and that the intersections of the regressions happen in the first quadrant.

On Fig. 7 — B it is possible to observe that unlike with the varying concentrations of NAD^+, 0.05 mg/mL of 1,5-diCQA had a smaller inhibitory effect than 0.025 mg/mL when the concentration of ethanol was varied and that the interception of the linear regressions is inside the first quadrant.

The effects of 5-CQA (Fig. 7 — C) follow the patterns of 1,3 and 1,5-diCQA with the lower concentration of 5-CQA having a higher slope.

3.2.2. Lactate dehydrogenase

The initial IC50 assays of lactate dehydrogenase using 3,4 and 3,5-diCQA as inhibitors did not present an acceptable linearity ($R^2 > 0.8$) when increasing the concentration of CQA (data not shown).

Due to the limited quantity of diCQAs, it would not be possible to perform new IC50 assays as well as the enzyme kinetics assays with these two diCQAs. Considering the main goal of this study, the kinetic assays were favored and the second set of IC50 assays was not performed.

The effects of 3,4-diCQA on lactate dehydrogenase with a variable concentration of NAD^+ were unexpected (Fig. 8 — A) as the lower concentration of diCQA reduced the slope of the regression when compared with the reaction without 3,4-diCQA.

It is also worth mentioning that the interception of the three regressions is in the first quadrant. When this assay was repeated (data not shown) the higher concentration of 3,4-diCQA caused a decrease in the slope of the reaction while the lower concentration of 3,4-diCQA caused an increase in the slope when compared to the reaction without 3,4-diCQA. In addition, the interception of these regressions was inside the second quadrant, characteristic of mixed inhibition.

The effects of 3,5-diCQA on lactate dehydrogenase with a variable concentration of NAD^+ are shown in Fig. 8 — B. When observing Fig. 8 — B it is possible to see that an increase in the concentration of 3,5-diCQA leads to an increase in the slope of the regression. It is also possible to observe that the two concentrations of 3,5-diCQA intercept the regression of the uninhibited reaction at different points. While the lowest concentration of 3,5-diCQA appears to exhibit competitive inhibition (interception at the vertical axis), the highest concentration of 3,5-diCQA intercepts the uninhibited reaction regression in the first quadrant. This behavior was also observed when this assay was repeated (data not shown).

When studying the effects of 5-CQA on NAD^+ kinetics (Fig. 8 — C), it is possible to observe once again uncharacteristic behavior. The highest concentration of inhibitor led to a smaller increase in slope than the lowest concentration of inhibitor.

The interception of all regressions lies in the first quadrant. However, when repeating this assay (data not shown) it was not possible to make the same observations as the data points were too far scattered making

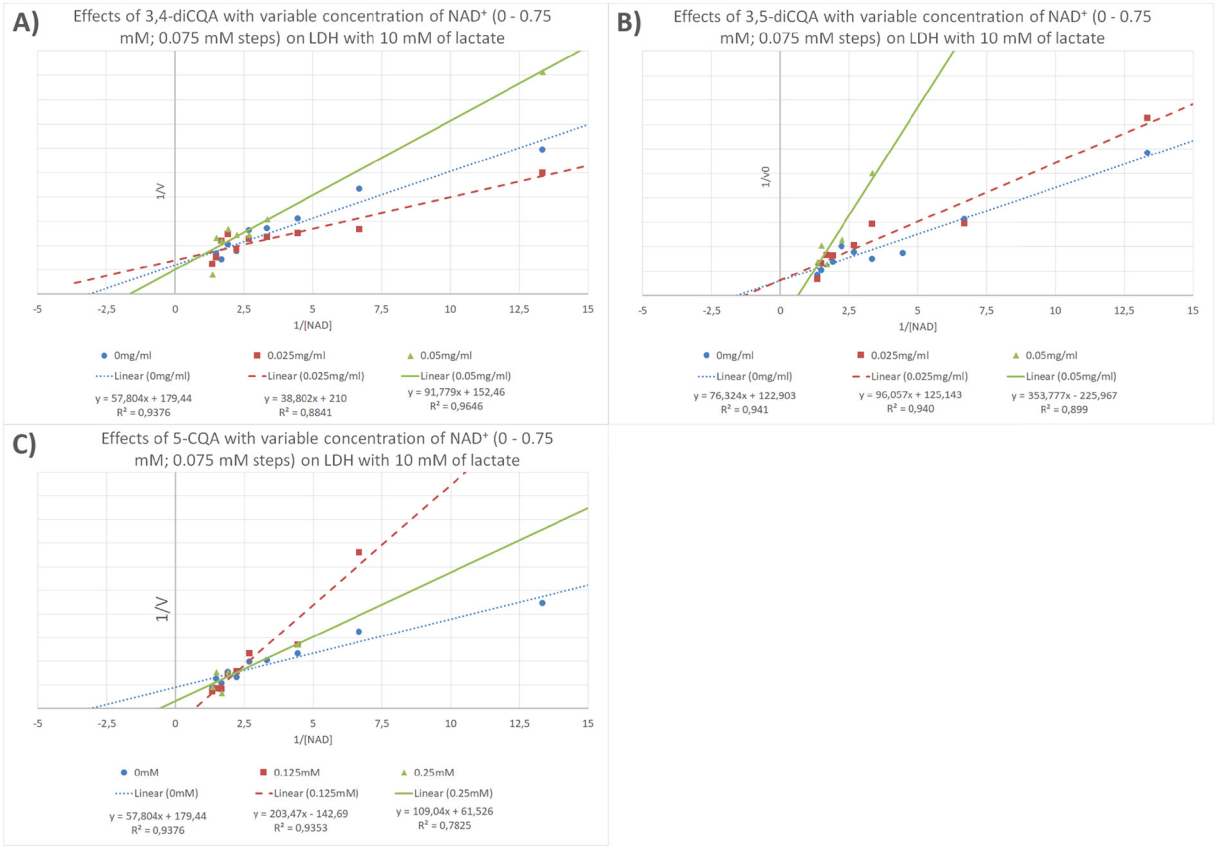

Fig. 8. Effects of CQAs on LDH and NAD^+ Kinetics: A) Effects of 3,4-diCQA with variable concentration of NAD^+ (0–0.75 mM; 0.075 mM steps) on LDH with 10 mM of lactate; B) Effects of 3,5-diCQA with variable concentration of NAD^+ (0–0.75 mM; 0.075 mM steps) on LDH with 10 mM of lactate.; C) Effects of 5-CQA with variable concentration of NAD^+ (0–0.75 mM; 0.075 mM steps) on LDH with 10 mM of lactate.

it impossible to perform a linear regression with an acceptable regression coefficient ($R^2 > 0.8$).

The results of 3,4-diCQA on lactate kinetics can be seen on Fig. 9 - A. An increase in the concentration of 3,4-diCQA lowered the slope of the regression.

When the assay was repeated (data not shown), the increase in CQA concentration led to an increase in the slope of the regression when compared to the uninhibited reaction. As for the interception of the regressions, while the highest concentration of 3,4-diCQA still intercepted the uninhibited reaction in the first quadrant, the lower concentration of inhibitor exhibited competitive inhibition when considering experimental error (interception very close to the vertical axis). However, one of the main limitations of the repetition was that the regression coefficient (R^2) was worse and below par ($R^2 \approx 0.71$) for the measurements where 3,4-diCQA was present.

When analyzing the effects of 3,5-diCQA on lactate kinetics (Fig. 9 — B) the two concentrations of 3,5-diCQA exhibited different behaviors. While the lowest concentration appeared to have no inhibitory power (regression parallel to the uninhibited reaction) the highest concentration intercepted the uninhibited reaction's regression in the first quadrant. When the assay was repeated (data not shown) the behavior of the lowest concentration of inhibitor was replicated while the higher concentration of 3,5-diCQA exhibited a negative slope which was attributed to some form of experimental error and the assays were repeated a third time.

On the third repetition, both concentrations of inhibitor displayed mixed inhibition mechanism and the lower concentration of 3,5-diCQA had a smaller slope than the uninhibited reaction (data not shown).

Of all CQAs, 5-CQA was the least reproducible and had the worse regression coefficients for the reaction with CQA present (Fig. 9 — C).

In Fig. 9 — C, the interceptions of the regressions are on the first quadrant and the lowest concentration of 5-CQA caused a reduction in the slope while the higher concentration of 5-CQA caused an increase in the slope when compared to the reaction without 5-CQA. When this assay was repeated (data not shown) it was not possible to reproduce the effect of the highest concentration of 5-CQA or to even observe any linearity between the data points. The lowest concentration of 5-CQA still intercepted the uninhibited reaction in the first quadrant but had a higher slope than it.

Considering the unexpected observations up to this point, the validity of the protocol being used was questioned. As such, a new assay (Fig. 9 — D) was performed using oxalic acid (a known competitive inhibitor towards lactate) instead of a CQA. The goal of this assay was to find if the highly variable, hard to replicate behavior and results were an artifact of the protocol.

From Fig. 9 — D, it is clear that oxalic acid competed with the substrate (interception of the regressions with at or very close to the vertical axis), the regression coefficient is excellent for both concentrations of the inhibitor and, doubling the concentration of the inhibitor (from 10 to 20 mM) caused the slope to double as well. These results show that the method being used is appropriate for this system.

4. Discussion

Most of the results from the kinetic assays showed that the regression of the reactions where CQAs were present intercepted the uninhibited reaction well inside the first quadrant of the Lineweaver-Burk plots. Initially, this was attributed to some form of experimental error. This meant that CQAs were acting as competitive inhibitors and that due to the experimental errors the regressions were intercepting each other in the first quadrant.

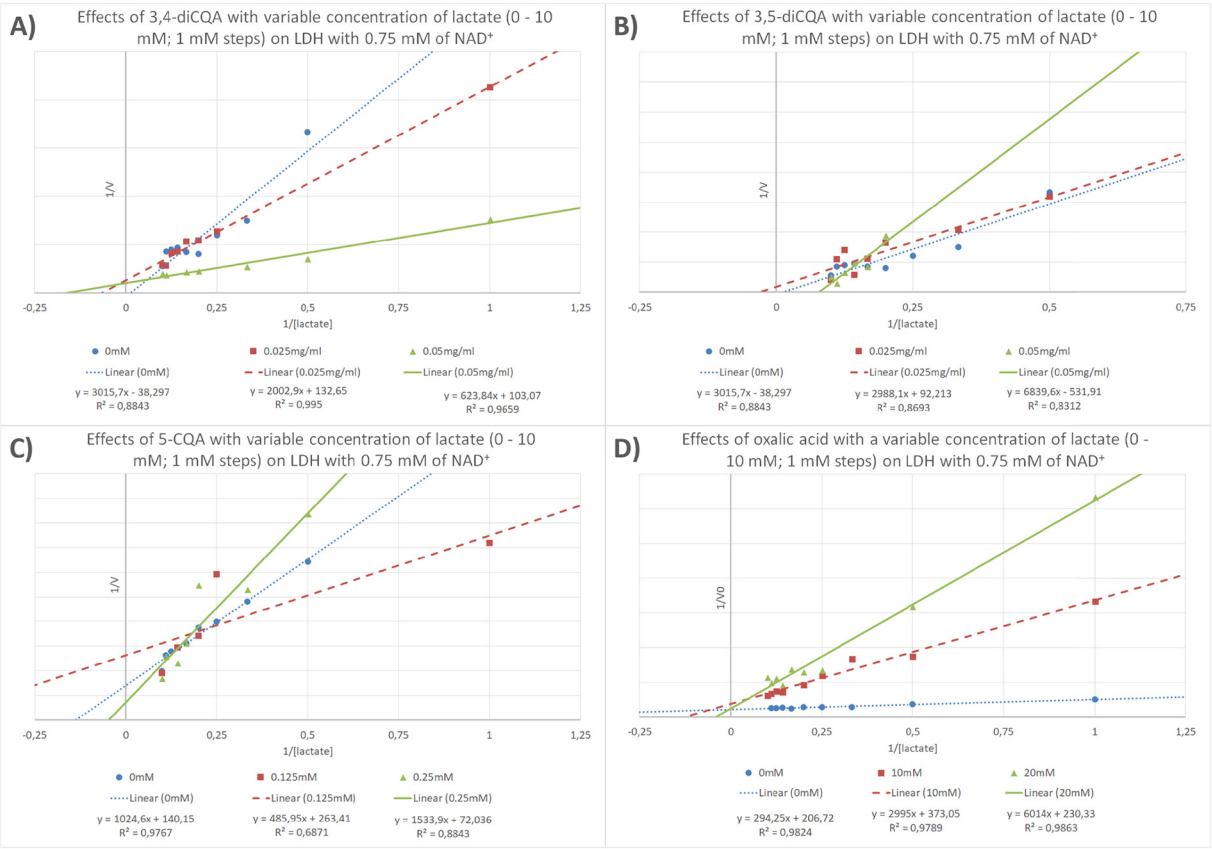

Fig. 9. Effects of CQAs and oxalic acid on LDH and lactate Kinetics: A) Effects of 3,4-diCQA with variable concentration of lactate (0–10 mM; 1 mM steps) on LDH with 0.75 mM of NAD^+; B) Effects of 3,5-diCQA with variable concentration of lactate (0–10 mM; 1 mM steps) on LDH with 0.75 mM of NAD^+; C) Effects of 5-CQA with variable concentration of lactate (0–10 mM; 1 mM steps) on LDH with 0.75 mM of NAD^+; D) Effects of oxalic acid with a variable concentration of lactate (0–10 mM; 1 mM steps) on LDH with 0.75 mM of NAD^+.

However, this behavior was still observed when the assays were repeated multiple times. Furthermore, while the cofactor and substrate sites are connected in LDH, in ADH they are separated. As such the hypothesis that the CQAs could compete with both molecules simultaneously was put aside. Masson et al. (Masson et al., 2008), studied butyrylcholinesterase and encountered a ligand that produced a similar Lineweaver-Burk plot to the ones from this work. According to the authors, this is a special case where the ligand can act as an inhibitor at low concentrations of the substrate but as an activator at high concentrations of the substrate. This mechanism of action would explain how CQAs are able to have a very high inhibitory effect in some enzymes of the carbohydrate metabolism with very low toxicity on healthy cells.

Nonetheless, it is imperative to recognize that this is merely an exploratory study of this topic and that further research is required. One of the main issues to overcome on further work is the method used to measure enzymatic activity/reaction progress. The caffeic acid moiety of CQAs has an absorption maximum at 325 nm that tails off up to approximately 360 nm (Spagnol et al., 2015). This inevitably interferes with the wavelength used to measure the concentration of NAD(H) and the reaction progress in these assays (340 nm). Even though the amount of available diCQAs was a limiting factor, the UV absorption of the caffeic acid moiety also limited the concentrations of diCQAs that could be used. Ideally, the reaction progress/quantification of each compound should be performed through chromatographic methods (HP/UP-LC). However, this might not always be feasible or available (as in our case) since the assay mix includes buffers, the enzyme and other components that are not usually safe to analyze using HP/UP-LC methods.

In summary, diCQAs appear to function as activators and inhibitors of NAD(P) dependent oxidoreductases of the glycolysis pathway. This mechanism of action appears to depend on their concentration and which isomer of diCQAs is being used. X-ray crystallography should be used to produce structures of these enzymes in the presence of CQAs to confirm their binding sites. Finally, more sophisticated quantification methods should be favored over simple spectroscopic methods due to the overlap in absorption peaks of NAD(P) with CQAs.

Acknowledgements

This research was supported by Fundação para a Ciência e a Tecnologia (FCT) with funds from the Portuguese Government (PEst-OE/QUI/UI0674/2013).

References

Bar-Even, A., Flamholz, A., Noor, E., Milo, R., 2012. Rethinking glycolysis: on the biochemical logic of metabolic pathways. Nature Chemical Biology 8:509–517. https://doi.org/10.1038/nchembio.971.

Bolaños, J.P., Almeida, A., Moncada, S., 2010. Glycolysis: a bioenergetic or a survival pathway? Trends in Biochemical Sciences 35:145–149. https://doi.org/10.1016/j.tibs.2009.10.006.

Cao, R., Zeidan, A.a., Rådström, P., Van Niel, E.W.J., 2010. Inhibition kinetics of catabolic dehydrogenases by elevated moieties of ATP and ADP — implication for a new regulation mechanism in Lactococcus lactis. FEBS Journal 277:1843–1852. https://doi.org/10.1111/j.1742-4658.2010.07601.x.

Conners, R., Schambach, F., Read, J., Cameron, A., Sessions, R.B., Vivas, L., Easton, A., Croft, S.L., Brady, R.L., 2005. Mapping the binding site for gossypol-like inhibitors of *Plasmodium falciparum* lactate dehydrogenase. Molecular and Biochemical Parasitology 142:137–148. https://doi.org/10.1016/j.molbiopara.2005.03.015.

Doherty, J.R., Cleveland, J.L., 2013. Targeting lactate metabolism for cancer therapeutics. The Journal of Clinical Investigation 123:3685–3692. https://doi.org/10.1172/JCI69741.transcription.

Feron, O., 2009. Pyruvate into lactate and back: from the Warburg effect to symbiotic energy fuel exchange in cancer cells. Radiotherapy and Oncology 92:329–333. https://doi.org/10.1016/j.radonc.2009.06.025.

Gibbons, B.J., Hurley, T.D., 2004. Structure of three class I human alcohol dehydrogenases complexed with isoenzyme specific formamide inhibitors. Biochemistry 43:12555–12562. https://doi.org/10.1021/bi0489107.

Haseba, T., Sugimoto, J., Sato, S., Abe, Y., Ohno, Y., 2008. Phytophenols in whisky lower blood acetaldehyde level by depressing alcohol metabolism through inhibition of alcohol dehydrogenase 1 (class I) in mice. Metabolism: Clinical and Experimental 57:1753–1759. https://doi.org/10.1016/j.metabol.2008.09.003.

Jelski, W., Kutylowska, E., Laniewska-Dunaj, M., Orywal, K., Laszewicz, W., Szmitkowski, M., 2011. Alcohol dehydrogenase (ADH) isoenzymes and aldehyde dehydrogenase (ALDH) activity in the sera of patients with acute and chronic pancreatitis. Experimental and Molecular Pathology 91:631–635. https://doi.org/10.1016/j.yexmp.2011.06.008.

Jelski, W., Laniewska-Dunaj, M., Orywal, K., Kochanowicz, J., Rutkowski, R., Szmitkowski, M., 2014. The activity of alcohol dehydrogenase (ADH) isoenzymes and aldehyde dehydrogenase (ALDH) in the sera of patients with brain cancer. Neurochemical Research 39:2313–2318. https://doi.org/10.1007/s11064-014-1402-3.

Kanehisa, M., Sato, Y., Kawashima, M., Furumichi, M., Tanabe, M., 2016. KEGG as a reference resource for gene and protein annotation. Nucleic Acids Research 44:D457–D462. https://doi.org/10.1093/nar/gkv1070.

Kanehisa, M., Furumichi, M., Tanabe, M., Sato, Y., Morishima, K., 2017. KEGG: new perspectives on genomes, pathways, diseases and drugs. Nucleic Acids Research 45:D353–D361. https://doi.org/10.1093/nar/gkw1092.

Lai, C.-L., Li, Y.-P., Liu, C.-M., Hsieh, H.-S., Yin, S.-J., 2013. Inhibition of human alcohol and aldehyde dehydrogenases by cimetidine and assessment of its effects on ethanol metabolism. Chemico-Biological Interactions 202:275–282. https://doi.org/10.1016/j.alcohol.2013.09.001.

Lee, Y.P., Liao, J.T., Cheng, Y.W., Wu, T.L., Lee, S.L., Liu, J.K., Yin, S.J., 2013. Inhibition of human alcohol and aldehyde dehydrogenases by acetaminophen: assessment of the effects on first-pass metabolism of ethanol. Alcohol 47:559–565. https://doi.org/10.1016/j.alcohol.2013.09.001.

Lee, S.-L., Lee, Y.-P., Wu, M.-L., Chi, Y.-C., Liu, C.-M., Lai, C.-L., Yin, S.-J., 2015. Inhibition of human alcohol and aldehyde dehydrogenases by aspirin and salicylate: assessment of the effects on first-pass metabolism of ethanol. Biochemical Pharmacology 95:71–79. https://doi.org/10.1016/j.alcohol.2013.09.001.

Lenzen, S., 2014. A fresh view of glycolysis and glucokinase regulation: history and current status. The Journal of Biological Chemistry 289:12189–12194. https://doi.org/10.1074/jbc.R114.557314.

Lineweaver, H., Burk, D., 1934. The determination of enzyme dissociation constants. Journal of the American Chemical Society 56:658–666. https://doi.org/10.1021/ja01318a036.

Masson, P., Froment, M.-T., Gillon, E., Nachon, F., Lockridge, O., Schopfer, L.M., 2008. Kinetic analysis of effector modulation of butyrylcholinesterase-catalysed hydrolysis of acetanilides and homologous esters. FEBS Journal 275:2617–2631. https://doi.org/10.1111/j.1742-4658.2008.06409.x.

Morris, G.M., Huey, R., Lindstorm, W., Sanner, M.F., Belew, R.K., Goodsell, D.S., Olson, A.J., 2009. AutoDock tools. Journal of Computational Chemistry 16:2785–2791. https://doi.org/10.1002/jcc.21256.

Niederhut, M.S., Gibbons, B.J., Perez-Miller, S., Hurley, T.D., 2001. Three-dimensional structures of the three human class I alcohol dehydrogenases. Protein Science: A Publication of the Protein Society 10:697–706. https://doi.org/10.1110/ps.45001.

Nordling, E., Jörnvall, H., Persson, B., 2002a. Medium-chain dehydrogenases/reductases (MDR). European Journal of Biochemistry 269:4267–4276. https://doi.org/10.1046/j.1432-1033.2002.03114.x.

Nordling, E., Persson, B., Jornvall, H., 2002b. Differential multiplicity of MDR alcohol dehydrogenases: enzyme genes in the human genome versus those in organisms initially studied. Cellular and Molecular Life Sciences 59:1070–1075. https://doi.org/10.1007/s00018-002-8487-6.

Ogata, H., Goto, S., Sato, K., Fujibuchi, W., Bono, H., Kanehisa, M., 1999. KEGG: Kyoto encyclopedia of genes and genomes. Nucleic Acids Research 27:29–34. https://doi.org/10.1093/nar/27.1.29.

Pelicano, H., Martin, D.S., Xu, R.-H., Huang, P., 2006. Glycolysis inhibition for anticancer treatment. Oncogene 25:4633–4646. https://doi.org/10.1038/sj.onc.1209597.

Powers, J.L., Kiesman, N.E., Tran, C.M., Brown, J.H., Bevilacqua, V.L.H., 2007. Lactate dehydrogenase kinetics and inhibition using a microplate reader. Biochemistry and Molecular Biology Education 35:287–292. https://doi.org/10.1002/bmb.74.

Quaytman, S., Schwartz, S.D., 2009. Comparison studies of the human heart and bacillus stearothermophilus LDH by transition path sampling. The Journal of Physical Chemistry. A 113, 1892–1897.

Serina, J., Castilho, P.C., Fernandes, M.X., 2016. Caffeoylquinic acids as inhibitors for HIV-I protease and HIV-I integrase. A Molecular docking study. SDRP Journal of Computational Chemistry & Molecular Modelling 1.

Spagnol, C.M., Oliveira, T.S., Isaac, V.L.B., Corrêa, M.A., Salgado, H.R.N., 2015. Validation of caffeic acid in emulsion by UV-spectrophotometric method. Physical Chemistry 5:16–22. https://doi.org/10.5923/j.pc.20150501.03.

Taber, R.L., 1998. The competitive inhibition of yeast alcohol dehydrogenase by 2,2,2-trifluoroethanol. Biochemical Education 26:239–242. https://doi.org/10.1016/S0307-4412(98)00073-9.

Trott, O., Olson, A.J., 2010. AutoDock Vina. Journal of Computational Chemistry 31:445–461. https://doi.org/10.1002/jcc.21334.

Venkataramaiah, T.H., Plapp, B.V., 2003. Formamides mimic aldehydes and inhibit liver alcohol dehydrogenases and ethanol metabolism. The Journal of Biological Chemistry 278:36699–36706. https://doi.org/10.1074/jbc.M305419200.

Walenta, S., Mueller-Klieser, W.F., 2004. Lactate: mirror and motor of tumor malignancy. Seminars in Radiation Oncology 14:267–274. https://doi.org/10.1016/j.semradonc.2004.04.004.

Warburg, O., 1956. On the origin of cancer cells. Science 123, 309–314.

Wiwanitkit, V., 2007. Plasmodium and host lactate dehydrogenase molecular function and biological pathways: implication for antimalarial drug discovery.

Chemical Biology & Drug Design 69:280–283. https://doi.org/10.1111/j.1747-0285.2007.00495.x.

Yu, Y., Deck, J. a., Hunsaker, L. a., Deck, L.M., Royer, R.E., Goldberg, E., Vander Jagt, D.L., 2001. Selective active site inhibitors of human lactate dehydrogenases A4, B4, and C4. Biochemical Pharmacology 62, 81–89. https://doi.org/10.1016/S0006-2952(01)00636-0.

Zengin, G., Uysal, A., Aktumsek, A., Mocan, A., Mollica, A., Locatelli, M., Custodio, L., Neng, N.R., Nogueira, J.M.F., Aumeeruddy-Elalfi, Z., Mahomoodally, M.F., 2017. *Euphorbia denticulata* Lam.: a promising source of phyto-pharmaceuticals for the development of novel functional formulations. Biomedicine and Pharmacotherapy 87:27–36. https://doi.org/10.1016/j.biopha.2016.12.063.